Toward defining plasma treatment dose : the role of plasma treatment energy of pulsed-dielectric barrier discharge in dictating in vitro biological responses

Plasma Processes and Polymers

Towards Defining Plasma Treatment Dose: The Role of Plasma Treatment Energy of Pulsed-Dielectric Barrier Discharge in Dictating in vitro Biological Responses

Journal:	*Plasma Processes and Polymers*
Manuscript ID	ppap.202100151.R1
Wiley - Manuscript type:	Research Article
Date Submitted by the Author:	n/a
Complete List of Authors:	Lin, Abraham; University of Antwerp, PLASMANT; University of Antwerp, Center for Oncological Research—Integrated Personalized & Precision Oncology Network (IPPON) Biscop, Eline; University of Antwerp, PLASMANT; University of Antwerp, Center for Oncological Research—Integrated Personalized & Precision Oncology Network (IPPON) Gorbanev, Yury; University of Antwerp, PLASMANT Smits, Evelien; University of Antwerp, Center for Oncological Research—Integrated Personalized & Precision Oncology Network (IPPON) Bogaerts, Annemie; University of Antwerp, PLASMANT
Keywords:	

Article type: Research Article

Title: Towards Defining Plasma Treatment Dose: The Role of Plasma Treatment Energy of Pulsed-Dielectric Barrier Discharge in Dictating *in vitro* Biological Responses

Abraham Lin[1,2*], Eline Biscop[1,2], Yury Gorbanev[1], Evelien Smits[2] and Annemie Bogaerts[1]

[1] PLASMANT-Research Group, University of Antwerp, Antwerp, Belgium
[2] Center for Oncological Research—Integrated Personalized & Precision Oncology Network (IPPON), University of Antwerp, Antwerp, Belgium

*Abraham Lin,
Email: Abraham.lin@uantwerpen.be

Abstract

The energy dependence of a pulsed-dielectric barrier discharge (DBD) plasma treatment on chemical species production and biological responses was investigated. We hypothesized that the total plasma energy delivered during treatment encompasses the influence of major application parameters. A microsecond-pulsed DBD system was used to treat three different cancer cell lines, and cell viability was analyzed. The energy per pulse was measured, and the total plasma treatment energy was controlled by adjusting pulse frequency, treatment time, and application distance. Our data suggest that the delivered plasma energy plays a predominant role in stimulating a biological response *in vitro*. This work aids in making steps toward defining a plasma treatment unit and treatment dose for biomedical and clinical research.

Keywords: non-thermal plasma; plasma energy; plasma medicine; plasma treatment dose; cancer treatment

1 INTRODUCTION

Non-equilibrium, atmospheric pressure plasma technologies are continually being investigated for biomedical applications, including haemostasis [1, 2], wound healing [3, 4], dentistry [5], surface sterilization [6], neuroregeneration [7, 8], and cancer therapy [9-11]. These technologies are commonly referred to as cold atmospheric plasma (CAP) or non-thermal plasma (NTP) in the biomedical and clinical fields. The extensive range of reported plasma-induced biological effects has been attributed to the reactive oxygen and nitrogen species (RONS) generated by plasma [12-15], as well as the cellular phenomena, hormesis [16]. Hormesis emphasizes the dose dependence of an agent to have either a beneficial or detrimental biological effect. In the context of plasma treatment, this suggests that low dose plasma treatment could promote regenerative effects, while higher dose treatments could induce cytotoxicity [16]. Therefore, based on the medical application (e.g. wound healing, cancer treatment), it is critical to define the appropriate plasma treatment dose [16, 17].

To date, an appropriate plasma treatment unit has not been defined or standardized in the field of plasma medicine. A major challenge has been the plethora of plasma devices, setups, and settings currently in use. Over the years, two main classes of plasma devices have emerged as the predominantly used systems for biomedical applications: the pulsed-dielectric barrier discharge (DBD) and the plasma jet [18, 19]. Although there have been comparative studies of pulsed-DBD and plasma jet treatments for a predefined cellular response [20], a unifying dose parameter remains elusive due to the different configurations and dependencies of the systems, which subsequently affect RONS generation and delivery (Table 1). While both DBDs and plasma jets also produce varying degrees of low-level ultraviolet radiation and electric fields which can be affected by these parameters, it has been reported that these plasma components alone have negligible contributions to biological effects compared to the chemical species produced [21-23]. Therefore, identifying the major contributing parameters of these different plasma systems would be a major step towards defining plasma treatment dose.

Recently, our group has investigated the interaction mechanism of a microsecond-pulsed DBD plasma with cancerous cells. We determined a regime of plasma that induced immunogenic cancer cell death (ICD) [24], an attractive type of cell death for cancer immunotherapy [25]. A thorough examination of the RONS generated by the microsecond-pulsed DBD plasma was also performed, showing that the short-lived species (e.g. •OH, •NO, O/O_3) were most responsible for inducing cell death and increasing cancer immunogenicity [24]. Furthermore, we observed that the generation of RONS with the DBD plasma system increased linearly with pulse frequency or treatment time, when the other parameters were fixed. Taken together, we hypothesized that the plasma treatment energy encompasses the major influence of application parameters (Table 1, e.g. pulse frequency, duration, distance) for pulsed-DBD treatment and dictates *in vitro* biological response.

Table 1. Parameters that influence DBD and plasma jet treatment

PARAMETERS	**PULSED-DBD**	**PLASMA JET**
ELECTRICAL	Waveform, Voltage	Waveform, Voltage
APPLICATION	Pulse Frequency, Duration, Distance	Pulse Frequency, Duration, Distance, Flow rate

In the present study, we investigated the energy dependence of pulsed-DBD plasma treatment on RONS generation and biological response, specifically for cancer cell treatment. We measured the plasma power in a setting that closely resembles *in vitro* biological experiments, in order to determine the energy delivered per plasma pulse during treatment. The total energy of treatment was calculated based on the energy per pulse and the total number of delivered pulses. At higher treatment distances, the energy per pulse was reduced, so treatment time was increased to deliver the same plasma energy. Chemical measurements of RONS and biological analysis on three different cell lines were performed at a fixed treatment energy, while other parameters were adjusted. Our results showed that when pulsed-DBD plasma

treatment energy was fixed, an equivalent level of cancer cell survival was achieved, regardless of changes to several other parameters. This was similarly observed for the amount of RONS generated. Taken together, our data suggest that the plasma treatment energy encompasses the influence of major pulsed-DBD application parameters and dictates *in vitro* biological response. This has major implications towards defining a standardized plasma treatment unit and treatment dose for biomedical applications.

2 EXPERIMENTAL SECTION

2.1 Experimental Design

We hypothesized that the total plasma energy delivered during treatment encompasses the influence of major application parameters and dictates the production of chemical species and biological effects *in vitro*.

The objective of this study was to investigate the importance of application parameters individually (i.e. application distance, pulse frequency, treatment time) and plasma treatment energy collectively, on biological responses and generated chemical species. This was accomplished by 1) determining the energy per pulse of the DBD plasma during treatment of biological samples, 2) analysing cancer cell survival, and 3) measuring chemical species in liquid.

2.2 Microsecond-Pulsed Power Supply

A microsecond-pulsed DBD plasma system was chosen for this study, unless otherwise specified, based on our previous experience with this system for cancer treatment [26]. The power supply was custom built (Megaimpulse Ltd., Russia), producing a 2 µs pulse (~30 kV) with a rise time of 1—1.5 µs. This system has been shown to be effective for treatment of 3D tumors *in vitro* and *in vivo* [26]. Power measurements were performed on this DBD plasma system, and liquid chemistry and cell survival analysis were also done to determine the effects of different plasma application parameters (i.e. pulse frequency, treatment time, application distance, total energy). The output of the power supply was connected to a DBD electrode. This

copper electrode (1.5 cm diameter) was covered with a 0.5 mm fused-silica dielectric with a 1.2 cm diameter (Technical Glass, USA).

2.3 Power Measurements

To determine the plasma power during treatment of cells *in vitro*, voltage and current were measured (Figure 1a) when plasma was generated at 500 Hz between the DBD electrode and a 6-well plate on a grounded metal platform, to simulate treatment of biological samples (Figure 1b). While all experiments were carried out in a 24-well plate, power measurements were performed in a 6-well plate for ease of use. Since, all cell-culture well plates from Corning have the same bottom thickness of 1.27 mm, which would serve as an additional dielectric, the discharge was not affected by different plate formats. As the DBD system and electrodes were made with the intention for *in vivo* and clinical experiments, they were made to be maximally insulating from the operator and treatment subject. Further manipulation of this setup would compromise the integrity of the shielding and introduce potential safety risks, so we had to perform power measurements using external voltage and current monitors. The position of the electrode was fixed with a z-positioner. Voltage was measured with a 1000X high voltage probe (P6015A, Tektronix), and current was measured using a current monitor (4100, Pearson Electronics, Inc.). The voltage and current waveforms were recorded on an oscilloscope (DSOX1102G, Keysight) with a 50 ns sampling rate and averaging 64 pulses. Instantaneous power ($P(t)$) was determined from voltage and current: $P(t) = \mathrm{V(t)} \times I(t)$. Energy per pulse ($\varepsilon_{pulse}$) is defined as the integration of the instantaneous power over the period of the pulse (T): $\varepsilon_{pulse} = \int_0^T P(t)dt$. Therefore, we calculated the energy per pulse: $\varepsilon_{pulse} = \sum_{k=1}^{n} |\mathrm{V}_k(\mathrm{t}) \times \mathrm{I}_k(\mathrm{t})| \times \Delta\mathrm{t}$, where Δt was 50 nanoseconds and the number of recorded samples (n) was 2000. Furthermore, the energy per pulse from displacement current was measured when the high voltage pulse was applied to the DBD electrode without a surface to discharge on (30 mm above the bottom of the well). This value was subtracted from all energy measurements in

order to account for the contribution of displacement current. Taken together, the energy per pulse reported here (ε_{pulse}) is the energy per pulse of the measured discharge ($\varepsilon_{pulse(discharge)}$) minus that of the displacement current ($\varepsilon_{pulse(displacement)}$):

$$\varepsilon_{pulse} = \varepsilon_{pulse(discharge)} - \varepsilon_{pulse(displacement)} \quad (1)$$

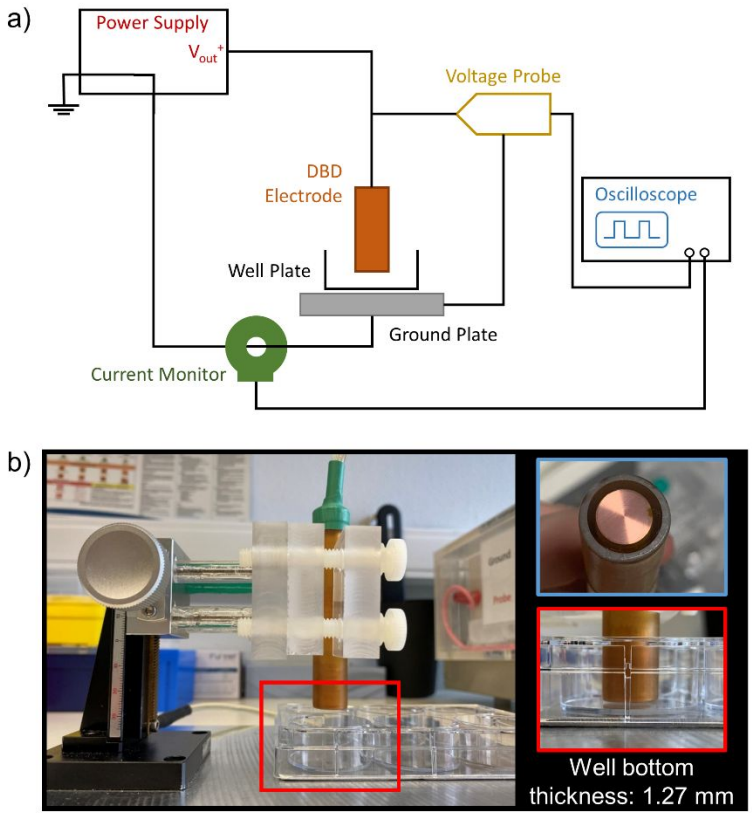

Figure 1. Experimental Setup. a) A schematic of the experimental setup to measure DBD plasma power is shown. b) A z-positioner was used to fix the position of the DBD electrode (blue insert) above the well for plasma treatment (red insert).

2.4 Chemical Measurements

The microsecond-pulsed DBD was used to treat 50 µL of phosphate-buffered saline (PBS) solution in a 24-well plate. The DBD electrode was positioned 1 mm above the liquid and plasma was generated in direct contact at varying pulse frequencies and treatment times. Following treatment, PBS was immediately collected and analysed for specific RONS. All chemical measurements were performed with at least 3 repeats on the same day.

2.4.1 H_2O_2 Measurements

A fluorometric assay kit (MAK165, Merck) was used according to the manufacturer's instructions to measure H_2O_2 concentration. As performed in our previous work [27], 25 µL of PBS treated with DBD plasma was added to each well, diluted with an equal amount of untreated PBS for a final volume of 50 µL. A master mix containing 4.75 mL Assay Buffer+50 µL Red Peroxidase Substrate+200 µL 20 units/mL Peroxidase, was then added to each well (50 µL) and samples were incubated for 30 minutes. Fluorescence was measured with the Tecan Spark Cyto (λex: 540 ± 20 nm, λem: 590 ± 20 nm, fixed gain 44).

2.4.2 NO_2^- and NO_3^- Measurements

A NO_2^-/NO_3^- colorimetric assay kit (780001, Cayman Chemical) was used for these experiments, following the developed protocols. NO_2^- was detected by adding 50 µL of Griess reagent 1 (sulphanilamide) to the DBD plasma-treated PBS in a 96-well plate, followed by immediately adding 50 µL of Griess reagent 2 (N-(1-naphthyl)ethylenediamine). In order to measure both NO_2^- and NO_3^- (NO_2^- + NO_3^-), a nitrate reductase mixture (780010, Cayman Chemical) and an enzyme cofactor mixture (780012, Cayman Chemical) were added to each sample and incubated for 1 h before the Griess reagent steps, thus allowing for the conversion of NO_3^- into NO_2^-. Due to the assay protocol and the small volumes treated, the concentrations of NO_2^- and NO_3^- were measured from independent experiments. An estimate of NO_3^- concentrations was therefore calculated by subtracting the mean NO_2^- concentration of each treatment condition from the NO_2^- + NO_3^- concentrations. Samples were prepared in triplicates, and the absorbance wavelength was measured at 540 nm using a Tecan Spark Cyto (20 readings per well). Concentrations of NO_3^- and NO_2^- were calculated from a calibration curve, obtained using standard solutions provided in the assay kit.

2.5 Biological Analysis

The microsecond-pulsed DBD was used to treat three cancer cell lines seeded in 24-well plates. Medium in the well was removed right before treatment, and the DBD electrode was positioned above the cells. Plasma was generated in direct contact with the cells at varying

distances, pulse frequencies, and treatment times, and fresh medium was replenished immediately after treatment.

2.5.1 Cell culture and treatment

A melanoma cell line (A375), a squamous cell carcinoma cell line (CAL-27), and a glioblastoma cell line (U87) were used in this experiment as they originate from different tissue, thus providing a broad overview of pulsed-DBD plasma effects without limitation to a single cancer type. All cell lines were cultured in Dulbecco's modified Eagle medium containing 10% fetal bovine serum, 100 U mL^{-1} penicillin, and 100 µL streptomycin. The melanoma media contained 4×10^{-3} M L-glutamine, while the other cell line media contained 2×10^{-3} M L-glutamine. All cells were cultured in a humidified environment at 37 °C with 5% CO_2 and plated in 24-well plates (150,000 cells/well) 1 day prior to DBD plasma treatment. Medium was removed from the well right before treatment, and the DBD electrode was lowered into the well and fixed at a position using a z-positioner (Figure 1b). Plasma was then discharged directly on the cells at parameters defined for each experiment. Following treatment, 500 µL of fresh medium was immediately replenished in the well and cells were immediately analyzed.

2.5.2 Cell survival assay

Cell survival was quantified immediately after DBD plasma treatment using the Trypan Blue exclusion test. Cell supernatant was collected from the wells, and the cells were washed with 200 µL of PBS. The PBS was also collected with the cell supernatant and 200 µL of Accutase was added to each well in order to detach the cells. The cell suspension, supernatant, and PBS wash was pooled together for each well and homogenized. In this way, all the cells were collected after DBD plasma treatment, and 20 µL of this cell suspension was acquired for cell counting. An equal part of 0.4% Trypan Blue (15250-061, Gibco) was added to each sample and counts were performed on an automated cell counter (TC20 Automated Cell Counter, Bio-Rad). Live cell concentrations were recorded, and survival reported here was a normalization of live cell counts to that of the untreated controls.

2.6 Statistical Analysis

Statistical differences for cell survival were analysed with JMP Pro 13 (SAS software) using the linear mixed model with treatment as the fixed effect. When the difference was significant ($P \leq 0.05$), an adjusted P value was calculated using the Dunnett's test when comparing to one group (e.g. untreated controls, 1 mm application distance), or the Tukey's test when comparing all conditions to each other. Measurements were performed on the same day for each chemical species, in at least triplicates. All *in vitro* experiments were performed in at least triplicates and repeated on separate days as independent replicates. For both *in vitro* experiments and chemical measurements, the total number of observations (n) is defined in the figure legend. A nonlinear regression using the least squares regression was performed for the chemical species measurements to determine linearity, using Graphpad Prism (Graphpad Software). The voltage and current plot was prepared using Python, and all other figures were prepared in Graphpad Prism (Graphpad Software). Data are represented as mean ± standard error of the mean (SEM) for *in vitro* experiments and mean ± standard deviation (SD) for chemical measurements.

3 RESULTS

3.1 Energy per Pulse of DBD Plasma

The energy of a single DBD discharge was calculated based on voltage and current measurements (Figure 2a) and after accounting for displacement current (details in Experimental Section). Since the physical and electrical properties of a material can affect the discharge characteristics of the plasma in contact with it [28], we measured the energy per pulse in an environment that most closely resembles treatment of biological samples. The DBD electrode was lowered into the well of a 6-well plate (polystyrene; 1.27 mm bottom thickness) and positioned 1 mm above the bottom, a commonly used position for DBD treatment *in vitro*. Since treatment of cells *in vitro* is never performed on dry samples, PBS was added into the well and then removed. Both the dry well and wet well (PBS added and removed before

discharge) conditions were tested. As commercial polystyrene cell culture plates are processed to be hydrophilic, which facilitates cell attachment, the PBS in the wet well appears to spread evenly along the bottom of the well and no visible aggregates were seen (Figure S1).

The energy per pulse for the wet and dry condition was found to be 1.88 mJ/pulse and 1.85 mJ/pulse, respectively, though they were not statistically different. Since the addition of the voltage probe could also affect the plasma energy, we tested whether this would have an effect on the biological response. A melanoma (A375), a head and neck squamous cell carcinoma (CAL-27), and a glioblastoma (U87) cell line were treated with the DBD plasma at 500 Hz for 10 seconds. The medium was removed immediately before treatment, and the DBD electrode was placed 1 mm above the cells. Plasma treatment was performed both without and with the voltage probe attached to the system, and cancer cell survival was measured. DBD treatment reduced survival of all three human cell lines, and the attachment of the probe did not significantly affect treatment (Figure 2b). Therefore, we concluded that the probe did not significantly change the measured plasma energy, and at 1 mm treatment, the discharge was ~1.88 mJ/pulse.

Since the application distance of the DBD electrode would change the applied electric field and thus potentially affect the power of the discharge, we investigated the distance dependence of the energy per pulse. The energy per pulse for both the wet and dry treatment conditions was similar for distances up to 4 mm (Figure 2c). At 5 mm we observed a decreasing trend, which was greater for the dry condition (0.56 ± 0.36 mJ/pulse) compared to the wet condition (1.44 ± 0.60 mJ/pulse), though this was not statistically significant. As distance increased, the average energy per pulse continued to decrease, but it appears that at relatively small application distances (≤ 4mm), the energy per pulse is approximately the same.

To test the influence of application distance during DBD plasma treatment on biological outcome, we treated the three human cancer cell lines with fixed plasma parameters (pulse frequency: 500 Hz; treatment time: 10 s) over a range of distances and measured cell survival.

Cell survival for all treatment conditions was compared to that of 1 mm application distance within the cell lines. Between 1 and 2 mm application distance, DBD plasma treatment did not significantly change cancer cell survival (Figure 2d). Cell survival deviated from that of the 1 mm treatment condition at 3 mm for CAL-27 and 4 mm for A375 and U87. For all cell lines, it was clear that at distances 4 mm and greater, cell survival was significantly affected, and by 10 mm, DBD plasma treatment had no effect on survival. This is most likely due to the decrease in the applied electric field as a result of the larger air gap, and consequently, a lowering of plasma treatment energy. Taken together, the biological results shown here (Figure 2d) compliment the electrical characterization of the DBD power supply (Figure 2c). For biological applications, *in vitro*, *in vivo* [29-31], and especially in the clinic [32-34], DBD plasma treatment is normally applied in close proximity to the target (1-2 mm), and therefore, subsequent experiments were performed with 1 mm distances unless otherwise specified.

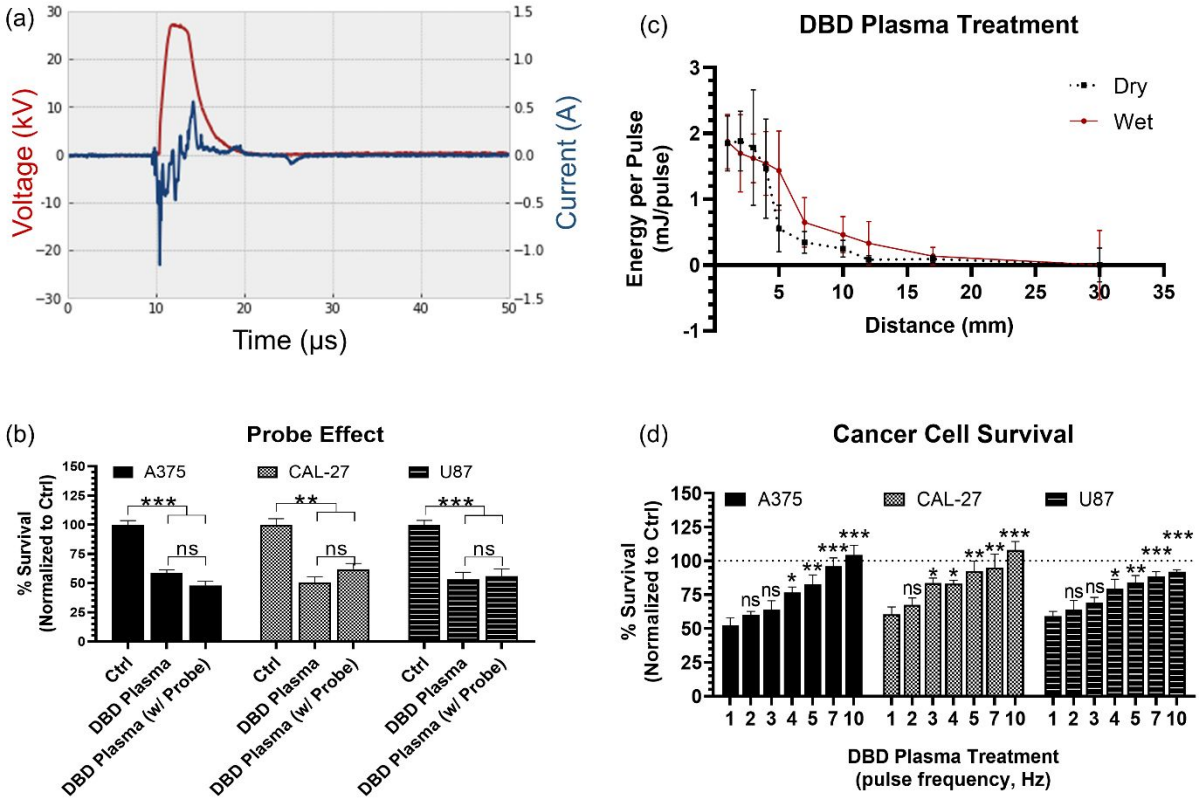

Figure 2. Electrical characterization of the DBD plasma system. a) Voltage and current waveform of a single DBD plasma discharge in a 6-well plate was measured on the oscilloscope. b) To determine if the attachment of the voltage probe significantly affected plasma power, the effect of plasma treatment on cancer cell survival was compared with and without the probe. DBD plasma treatment significantly

reduced cell survival of three cancer cell lines (melanoma, A375; squamous cell carcinoma, CAL-27; glioblastoma, U87), and no statistical difference was measured with and without the probe connected to the system (n=3-6). Treatment conditions were compared to each other to determine statistical significance. ns, $P \geq 0.05$; **, $P \leq 0.01$; ***, $P \leq 0.001$ (generalized linear mixed model, Tukey's test). c) The energy per pulse was calculated from the voltage and current waveform (see text) at different application distances for a dry and wet well. d) These results were correlated to cancer cell survival after treatment when the cells were exposed to DBD plasma at varying distances. All treatment conditions were compared to that of the 1 mm application distance to determine statistical significance (n=3-7). ns, $P \geq 0.05$; *, $P \leq 0.05$; **, $P \leq 0.01$; ***, $P \leq 0.001$ (generalized linear mixed model, Dunnett's test). Data here are represented as mean ± SEM.

3.2 Energy Dependence of DBD Plasma Treatment on Cancer Cell Survival

It is well documented that increasing plasma treatment duration or pulse frequency (particularly for direct pulsed-DBD plasma treatments) induces higher levels of cancer cell death [21, 24]. This was also demonstrated with our DBD plasma system (Figure S2). Here, we tested our hypothesis that cancer cell death is dependent on the delivered plasma treatment energy, and independent of a single parameter. The three cancer cell lines were exposed to DBD plasma, at a 1 mm distance, with a range of pulse frequencies (50─500 Hz) and application times (100─10 seconds). The number of delivered pulses was the same (5000 pulses) and the total delivered energy was calculated to be approximately 9.4 J based on the measured energy per pulse (Figure 1c).

Immediately after DBD plasma treatment, cells (and their supernatants) were collected, analyzed, and normalized to that of the untreated controls to obtain the percentage of cancer cell survival. DBD plasma treatment at 9.4 J reduced survival for all cell lines: 49 ± 3% for A375, 59 ± 5% for CAL-27, and 62 ± 2% for U87. Furthermore, no significant difference was measured between the different treatment times and pulse frequencies (Figure 3a). Interestingly, a similar response was demonstrated using a second microsecond-pulsed DBD plasma system (details in Supporting Information). Following exposure to plasma at an equivalent energy, two melanoma cell lines exhibited an increased immunogenicity marker, and no difference was measured between the different conditions (i.e. pulse frequencies and treatment times) when the delivered plasma energy was held constant (Figure S3). Taken together, these results highlight the importance of plasma treatment energy for anti-cancer activity.

Since both energy per pulse and cancer cell death decreased with application distance (Figure 2c, d), we also test our hypothesis that cell survival was dependent on the plasma treatment energy, by treating the three cancer cell lines at various distances while delivering equivalent energies. The pulse frequency of DBD plasma treatment was fixed at 500 Hz, the application distance was fixed at either 1, 5, 7, or 10 mm, and the treatment time was adjusted to 10, 13, 30, and 41 s, respectively, to deliver a total of 9.4 J, based on the energy measured in the wet condition (Figure 2c). The energies per pulse at different distances are detailed in the figure. Regardless of time and distance, when the NTP treatment energy was fixed to 9.4 J, equivalent cell survival was achieved between the treatment groups of all three cell lines (Figure 3b). While all treatments were able to reduce cell survival to 60 ± 4% (A375), 65 ± 2% (CAL-27), and 58 ± 3% (U87) compared to untreated controls, no differences were measured between treatment at different heights.

Therefore, we demonstrated that equivalent cell survival could be achieved when the delivered plasma treatment energy was the same, regardless of pulse frequency, treatment time, and application distance alone (Figure 3). Taken together, this strongly evidences the importance of pulsed-DBD plasma treatment energy to elicit cell death over a single application parameter.

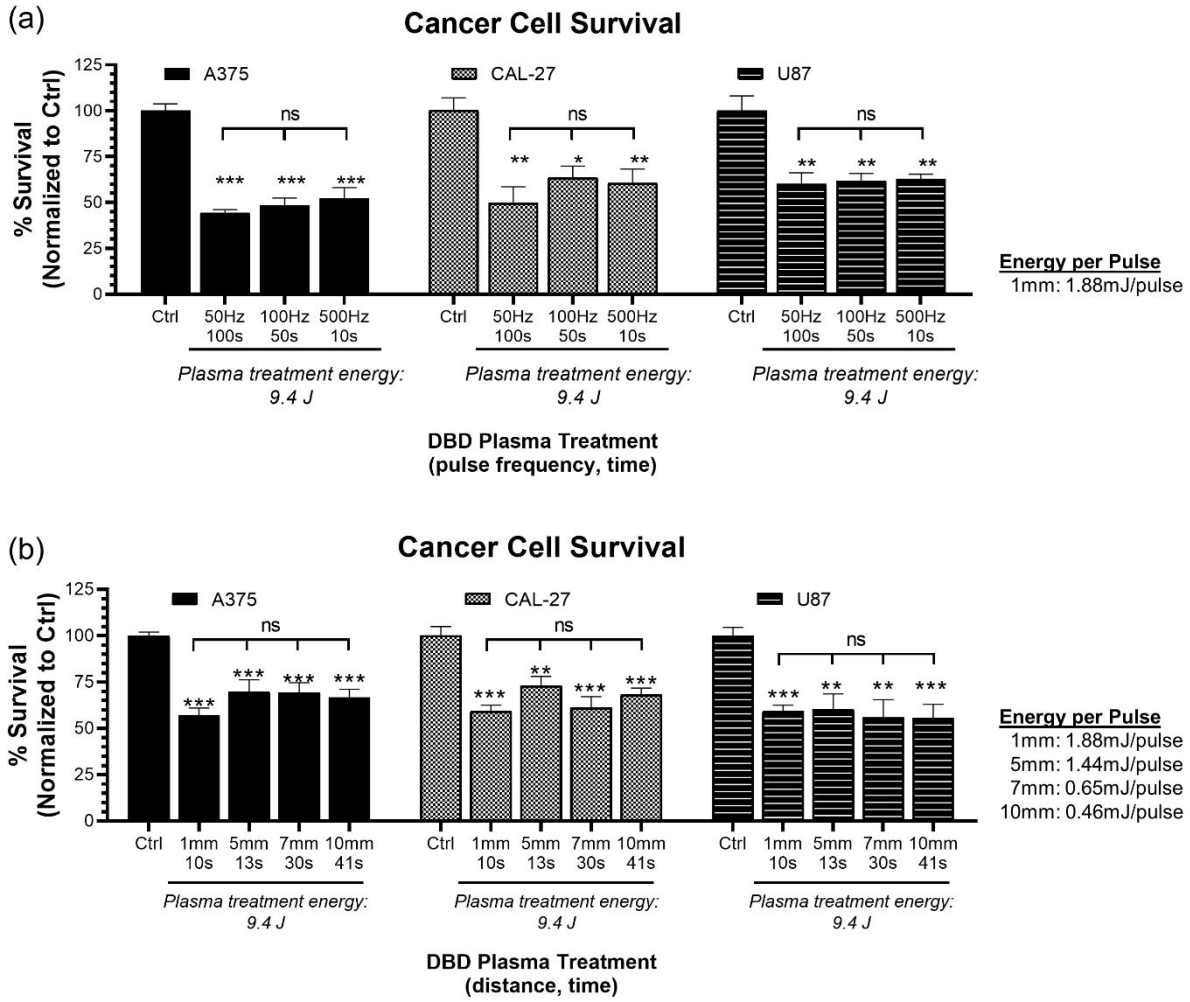

Figure 3. Energy dependence of DBD plasma treatment for cancer cell survival. a) Melanoma (A375), squamous cell carcinoma (CAL-27), and glioblastoma (U87) cells were exposed to 9.4 J of DBD plasma while varying pulse frequency and treatment duration (n=3-6). While all treatment conditions resulted in a significant decrease in percent survival compared to untreated controls, no difference was observed between the different conditions. b) The treatment time was extended at higher application distances, based on the drop in the energy per pulse, in order to deliver the same plasma treatment energy (9.4 J) to the cancer cells (n=5-12). While all treatments reduced cell viability compared to untreated controls, no differences were observed between treatments. Treatment conditions were compared to each other to determine statistical significance. ns, $P \geq 0.05$; **, $P \leq 0.01$; ***, $P \leq 0.001$ (generalized linear mixed model, Tukey's test). Data here are represented as mean ± SEM.

3.3 Energy Dependence of DBD Plasma Treatment for Generating Reactive Oxygen and Nitrogen Species

It is well-documented that plasma-generated RONS are the major effectors of biological response [13, 16, 21, 24]. Therefore, we also investigated how pulse frequency, treatment time, and treatment energy influence the generation of chemical species by DBD plasma in 50 µL of

PBS. H_2O_2 was measured using a fluorometric assay kit, and NO_2^- and NO_3^- were measured with the Griess method and a nitrate reductase enzyme and cofactor.

First, treatment time was fixed to 10 seconds and pulsed-DBD plasma was applied using a range of pulse frequencies (50, 100, 200, and 500 Hz), which correspond to 0.9, 1.9, 3.8, and 9.4 J treatment, respectively. Unsurprisingly, as pulse frequency (and subsequently treatment energy) increased, H_2O_2, NO_2^-, and NO_3^- concentrations increased linearly. H_2O_2 concentration increased linearly (R^2=0.85) up to 17.1 μM for 500 Hz (9.4 J) treatment (Figure 4a). NO_2^- and NO_3^- concentrations also increased similarly up to 42.8 and 69.4 μM for 500 Hz treatment, respectively (Figure 4b, c).

Next, to test the sole influence of treatment time on RONS generation, pulse frequency was fixed at either 50 Hz or 500 Hz, and plasma was applied over a range of treatment times (1, 5, 10, 50, 100 s). H_2O_2 concentrations for both 50 and 500 Hz increased linearly (R^2=0.91 and R^2=0.99, respectively) over time (Figure 4d). Similarly, the NO_2^- and NO_3^- concentration showed a linear increase with increasing treatment time for both pulse frequencies tested (Figure 4e, f). Therefore, within the range of pulse frequencies tested (and commonly used in the biomedical applications), RONS concentrations increase linearly over time.

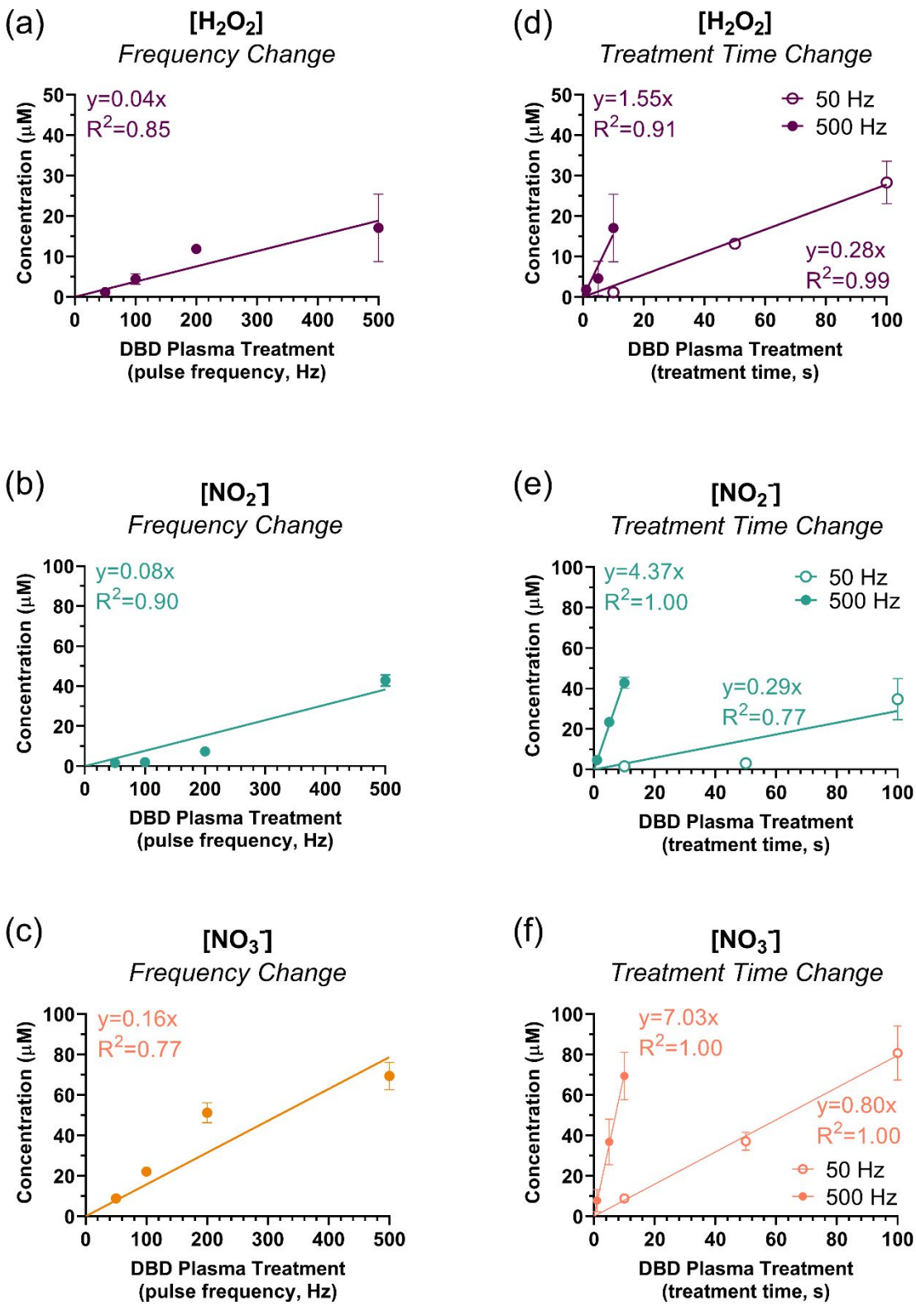

Figure 4. RONS concentration increased linearly with pulsed-DBD plasma treatment. Treatment was fixed at a distance of 1 mm for 10 seconds and a range of pulse frequencies were tested. a) H_2O_2, b) NO_2^-, and c) NO_3^- concentrations were measured in PBS immediately following treatment. Next, two pulse frequencies were chosen, and treatment time was adjusted. The d) H_2O_2, e) NO_2^-, and f) NO_3^- concentrations increased linearly with treatment time for both pulse frequency conditions. Data here are represented as mean ± SD (n=3-9).

Based on these results, it appeared that plasma treatment energy was also responsible for the generation of RONS. In fact, Figure 4a, b, c could be represented as a linear increase in plasma treatment energy (Figure 5a, b, c). To investigate this further, four frequencies were tested (50, 100, 200, and 500 Hz) and the treatment time was adjusted to deliver the same number of pulses (5000 pulses) during DBD plasma treatment, corresponding to 9.4 J treatment. Following all treatments, the H_2O_2 concentration was nearly equivalent (20.18 ± 7.9 μM), regardless of pulse frequency or treatment time (Figure 5d). The concentrations of NO_2^- (34.2 ± 8.7 μM) and NO_3^- (82.8 ± 15.4 μM) were also nearly equivalent when the number of NTP treatment energy was standardized (Figure 5e, f).

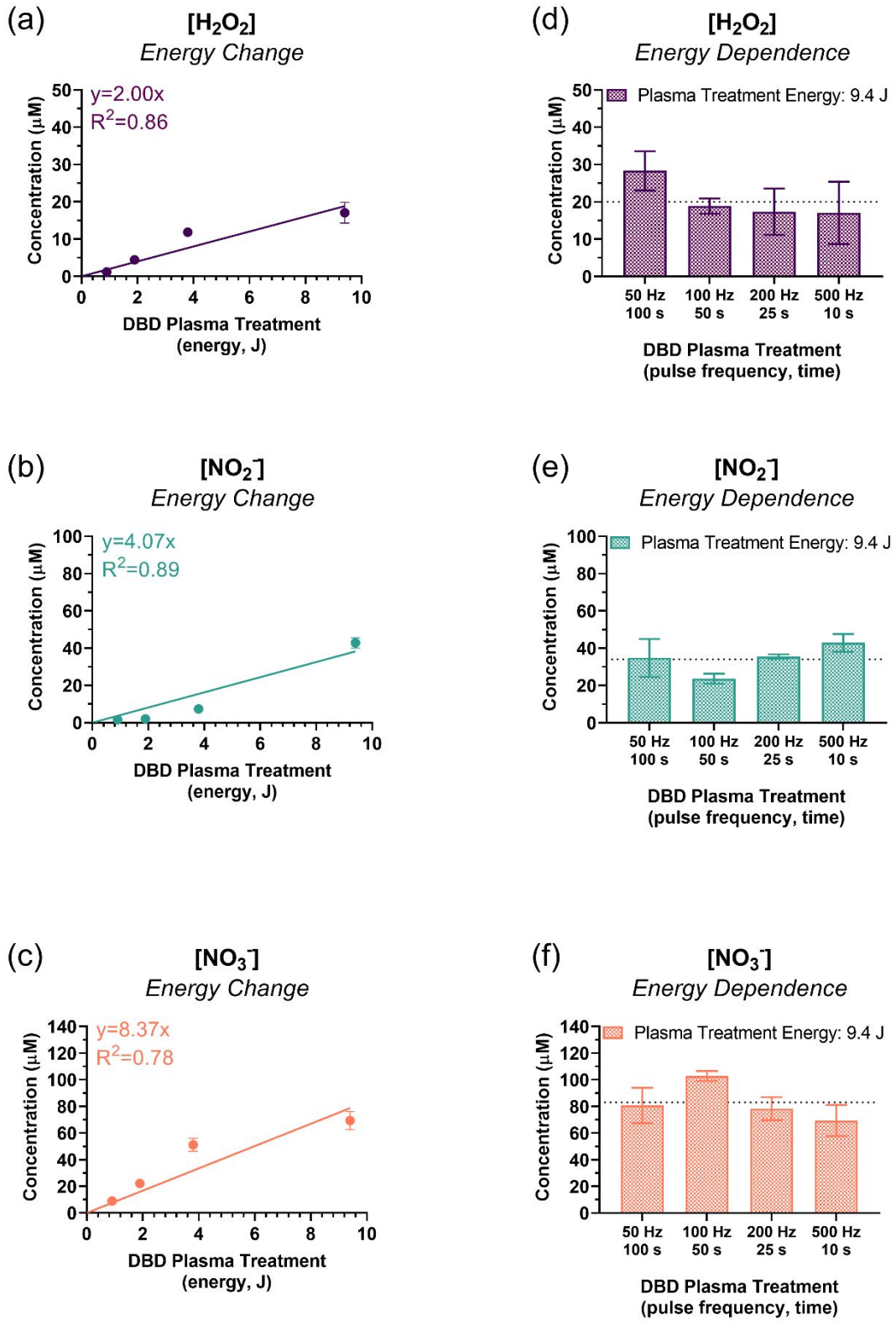

Figure 5. Energy dependence of DBD plasma treatment on RONS generation. a) H_2O_2, b) NO_2^-, and c) NO_3^- concentrations increased linearly in PBS when exposed to plasma at higher treatment energies. Regardless of pulse frequency or treatment time alone, when the total number of pulses was fixed, DBD plasma treatment produced nearly equivalent amounts of d) H_2O_2, e) NO_2^-, and f) NO_3^-. Data here are represented as mean ± SD (n=3-9), and the dotted line represents the mean concentration.

Altogether, it is clear that for DBD plasma-generated species measured here, neither pulse frequency nor application time alone was the major contributing parameter. Instead, the generation of RONS depended on the total delivered energy during treatment. This was also demonstrated with a second pulsed-DBD power supply, when a fixed number of pulses was delivered at a 1mm treatment distance. In addition to the persistent RONS measured here (H_2O_2, NO_2^-, and NO_3^-), short-lived RONS ($O/^1O_2/O_3$, and $ONOO^-$) were also analyzed following treatment. The concentrations of all these chemical species were equivalent when the total delivered energy was the same (Figure 6), suggesting that this could be used as an internal calibration for pulsed-DBD devices and RONS generation. A detailed reporting of the methods and results of this second power supply is provided in Supporting Information−Section 4.

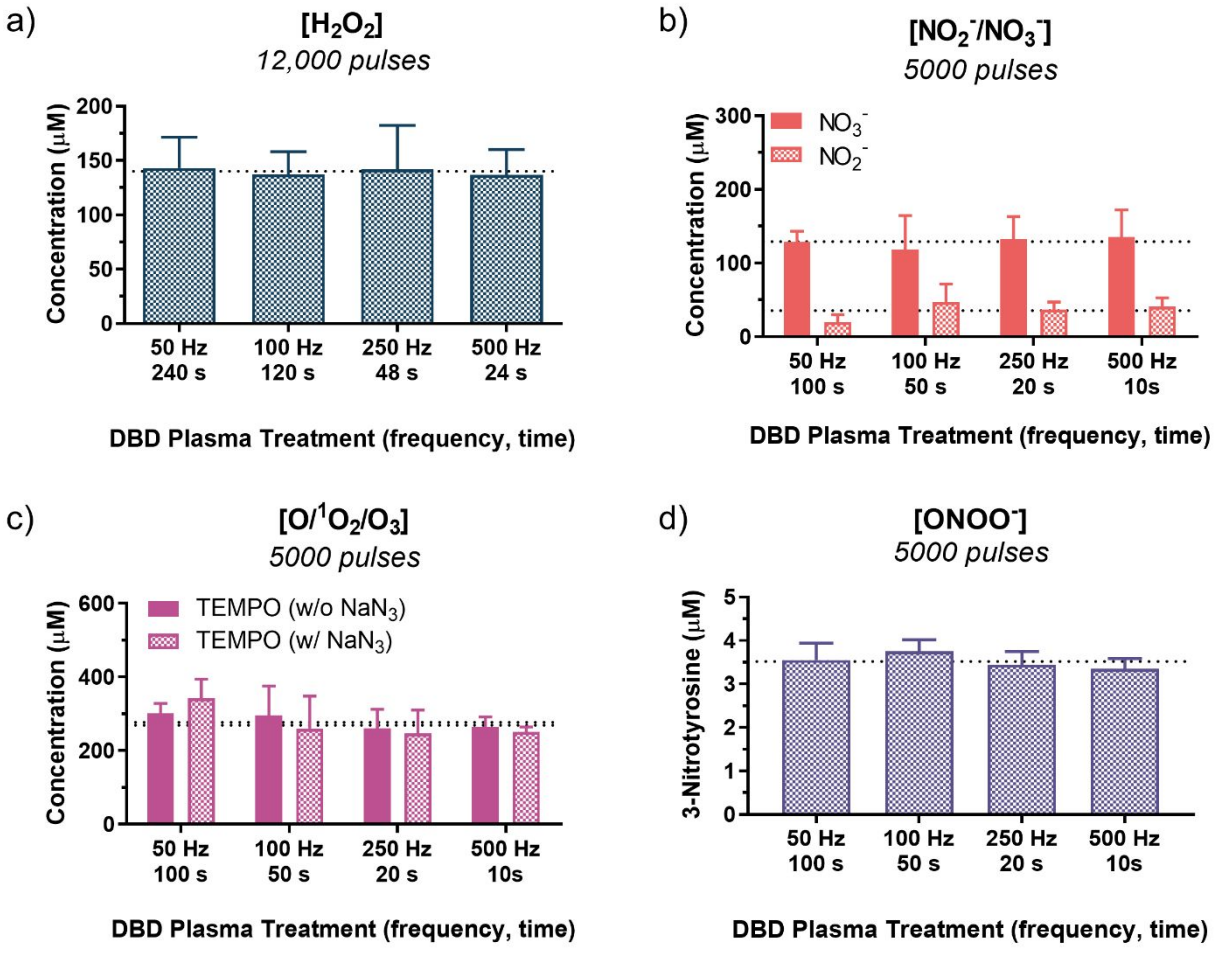

Figure 6. Chemical analysis of a second pulsed-DBD plasma system. PBS was treated in 24-well plates with equivalent DBD plasma treatment energy by delivering a fixed total number of pulses while pulse frequency and treatment duration was adjusted. a) H_2O_2 concentration (n=3-4) and b) NO_2^-/NO_3^- concentration (n=4-6) was measured by spectrophotometry. c) $O/_1O^2/O_3$ concentration (n=3-5) was

measured with EPR spectrometry, and d) $ONOO^-$ concentration (n=3) was measured by LC-MS. Regardless of pulse frequency or treatment time alone, when the total number of pulses, and thus treatment energy, was fixed, DBD plasma treatment produced equivalent amounts of all RONS measured here. Data are represented as mean ± SD, and the dotted line represents the mean concentration.

4 DISCUSSION

Research into the therapeutic properties of non-equilibrium, atmospheric pressure plasma is ongoing and covers a broad range of applications. However, the ability to quantify, predict, and control plasma treatment outcomes remains a challenge and a major obstacle for clinical translation. The sensitivity of plasma to its intrinsic characteristics (e.g. voltage, waveform), application parameters (e.g. pulse frequency, time, working distance), and environmental perturbations (e.g. gas composition, humidity, biological surface) also contributes to the complexity of this challenge. To streamline adoption of plasma technologies into the clinic, it is necessary to provide a method of standardizing treatment in a way that accounts for these different influences and results in a controllable and predictable therapeutic outcome. In this study, we investigated how application parameters could be standardized. We hypothesized that the delivered plasma energy encompasses the major application parameters for DBD plasma treatment and dictates biological responses.

We tested our hypothesis through electrical characterization of a microsecond-pulsed DBD system (in a pulse range commonly used *in vivo* and in the clinic) and by determining the energy dependence for generating chemical species and biological responses. Contrary to previous notions, we demonstrated that increasing treatment time alone does not lead to a more pronounced biological response, as other factors also play a role (Figure 2e, Figure 3). We have summarized the parameters tested and the resulting effects on cell survival when treatment was fixed at 9.4 J (Table 2). Regardless of treatment distance, exposure time, and pulse frequency, when cells were treated with 9.4 J of NTP, similar effects on cell viability were achieved. Here, we would like to emphasize that, while we do not believe treatment energy to be the single

decisive factor for biological response, it does encompass many of the application parameters (Table 1), thus making it a suitable candidate for further dose standardization development.

Table 2. Treatment of cells at an equivalent total NTP energy resulted in similar cell viability, independent of a single parameter

TOTAL NTP TREATMENT ENERGY (J)	TREATMENT DISTANCE (MM)	TREATMENT TIME (S)	PULSE FREQUENCY (HZ)	DELIVERED PULSES (PULSES)	A375 VIABILITY (%)	CAL-27 VIABILITY (%)	U87 VIABILITY (%)
9.4	1	10	500	5000	52 ± 6	61 ± 8	63 ± 3
	1	50	100	5000	48 ± 4	64 ± 6	62 ± 4
	1	100	50	5000	44 ± 2	50 ± 9	60 ± 8
9.4	1	10	500	5000	57 ± 4	59 ± 3	59 ± 3
	5	13	500	6500	70 ± 6	73 ± 5	60 ± 8
	7	30	500	15000	70 ± 5	61 ± 6	56 ± 9
	10	41	500	20500	67 ± 4	68 ± 3	56 ± 7

The pulsed-DBD system was operated at atmospheric pressure and in air, which is mainly composed of 78% nitrogen and 21% oxygen. In the past, it has been reported that the oxygen molecules in air are the main effectors for both reducing cell survival and increasing cancer immunogenicity [13, 21]. When air was flushed out and replaced with pure oxygen during *in vitro* treatment of different cell types, cell death and even immunogenic cell death was equivalent to those treated in air. When pulsed-DBD treatment was performed in pure nitrogen, no differences were observed compared to the controls. Taken together, this suggests that while DBD treatments are influenced by gas composition, they are not as sensitive as plasma jets, and a minimum threshold of oxygen molecules is needed to achieve a biological response. Furthermore, as the composition of air remains relatively the same and in the clinical context, hospital settings are further controlled, dramatic changes to air composition that would affect DBD treatment (and associated changes to discharge energy) seem unlikely.

It has been reported that the surface of treatment can greatly affect plasma discharge [13, 28]. Lin et al., and Simoncelli et al., have shown that electrical power is higher for plasma discharges on metal compared to a dielectric for both DBDs and plasma jets, respectively. Since plasma treatments in this study for all chemical and biological analyses were performed in

polystyrene well plates, the energy per pulse of DBD plasma was calculated in a setting that closely resembles these experiments (Figure 1). Furthermore, we demonstrated that as the application distance of plasma treatment was increased, the energy per pulse was reduced (Figure 2c). DBD plasma treatment of three human cancer cell lines also revealed the same trend in cell survival (Figure 2d), though no statistically significant differences were observed at relatively small distances (1-3 mm). While these small changes in distance may affect the aqueous species generated, they did not significantly affect biological response. Furthermore, we demonstrated that equivalent cell survival could be achieved following NTP treatment of the cell lines at various distances if treatment time was also adjusted to deliver the same energy (Figure 3). Interestingly, this shows that treatment is not limited to short distances, as long as the total treatment energy required for a biological response can be delivered. Taken together, this suggests that the plasma treatment energy also accounts for the working distance parameter.

We recognize several limitations of our study, mainly due to the limitations of our power supply. Since the voltage and waveform of the power supply could not be changed, we were unable to test how these could affect treatment energy and subsequent chemical and biological responses. When looking into previous reports where the energy of *in vitro* treatment was defined, we see that these parameters indeed contribute to the measured energy per pulse [20, 35, 36]. Therefore, it may be that as pulsed-DBD systems transition into the clinic, the plasma treatment range must be standardized for each device. Furthermore, it would be of interest to investigate how the discharge develops in the different systems, with varying treatment parameters, while keeping the total delivered energy constant. Indeed, we have identified similar trends in a separate microsecond-pulsed DBD power supply on biological response (Figure S3) and the generation of RONS (Figure 6), but more in-depth investigation and broad applicability still must be tested. Furthermore, future translation of plasma technology might need to consider the area or mass of the treatment target, similar to how radiotherapy doses are

defined today. However, taken together, this provides insight into how pulsed-DBD plasma treatment energy could be used to standardize plasma therapy for cancer applications.

Progress towards standardizing plasma treatment dose is critically needed for wide clinical adoption of plasma medicine technologies, and work towards a plasma treatment unit has also been proposed [37]. Recently, Cheng et al. has also suggested an equivalent total oxidation potential (ETOP) as a means to summarize plasma treatment dose [38]. In this paper, the authors have provided an equation that relies on several factors including oxidation potential of various species, average number density and velocity of the species, cross section of plasma interaction area, and treatment time. They have correlated this ETOP to bacterial reduction for several plasma jets, but further practical and clinical considerations are still required, including how the application parameters affect ETOP.

Still another challenge that must be addressed to overcome this barrier for clinical adoption includes the reproducibility of treatment. Current devices in the clinic are handheld and operated by the clinician and therefore, rely heavily on the clinician's judgment [3, 4, 32, 39-43]. Consequently, this leads to large variability, which is further amplified when the ratio of treatment area to the plasma applicator is large, and the plasma applicator must be translated across the field for complete treatment. These challenges are not exclusive to plasma treatment and have also been faced by radiation technology [44-46]. Therefore, implementation of solutions from radiotherapy could also greatly benefit plasma technology. For example, real-time tumor tracking is a recent methodology that actively counteracts tumor wandering with compensatory motion of the source or the target [44, 47]. Gidon et al. and Bonzanini et al. have also investigated the use of machine learning and non-linear model-predictive control strategies to deliver a safe plasma dose [17, 48, 49]. They have aimed to quantify thermal dose and temperature changes on the plasma-treated surface, and it would be interesting to combine their work with the insight gained from our studies presented here. In fact, *in situ* measurement of deposited plasma treatment energy onto target cells or patient tissue with a feedback loop

control system would be highly valuable, and it is of high priority in our plan to bridge the gaps between preclinical and clinical studies.

In summary, we have demonstrated that the plasma treatment energy highly influenced RONS production and biological effect for *in vitro* cancer application. This suggests that plasma treatment energy encompasses the impact of other parameters (e.g. pulse frequency, treatment time) and warrants keen attention during translation of plasma medicine technologies. Still, more in-depth investigations into the energy dependency of DBD plasma treatment on other cancer-associated effects (e.g. type of cell death, senescence, epithelial-to-mesenchymal transition) is needed, as well as *in vivo* testing. However, overall, this work aids in making a vital step towards defining a plasma treatment unit and treatment dose, and these principles should also be investigated for other biomedical and therapeutic applications in plasma medicine as well (e.g. wound healing, neuroregeneration, surface sterilization).

ACKNOWLEDGMENTS

The authors would like to thank Karel Venken for his expertise and experience with the measurements of voltage and current profiles of plasma. We would like to thank Prof. Dr. Filip Lemière and Prof. Dr. Paul Cos for sharing their equipment. Finally, we would also like to thank Prof. Dr. Erik Fransen (StatUa Center for Statistics, University of Antwerp) for his help with the statistical analysis.

FINANCIAL DISCLOSURE

This study was funded in part by the Flanders Research Foundation (12S9218N, 12S9221N, G044420N).

CONFLICT OF INTEREST

The authors declare no financial or commercial conflict of interest.

DATA AVAILABILITY STATEMENT

The data that support the findings of this study are available from the corresponding author upon reasonable request.

REFERENCES

[1] M. Ueda, D. Yamagami, K. Watanabe, A. Mori, H. Kimura, K. Sano, H. Saji, K. Ishikawa, M. Hori, H. Sakakita, Histological and Nuclear Medical Comparison of Inflammation After Hemostasis with Non‐Thermal Plasma and Thermal Coagulation, Plasma Processes Polymers 12 (2015) 1338-1342.
[2] K. Miyamoto, S. Ikehara, H. Sakakita, Y. Ikehara, Low temperature plasma equipment applied on surgical hemostasis and wound healings, Journal of clinical biochemistry nutrition & Food Science 60 (2017) 25-28.
[3] G. Isbary, J. Heinlin, T. Shimizu, J. Zimmermann, G. Morfill, H.U. Schmidt, R. Monetti, B. Steffes, W. Bunk, Y. Li, Successful and safe use of 2 min cold atmospheric argon plasma in chronic wounds: results of a randomized controlled trial, British Journal of Dermatology 167 (2012) 404-410.
[4] S. Bekeschus, A. Schmidt, K.-D. Weltmann, T. von Woedtke, The plasma jet kINPen–A powerful tool for wound healing, Clinical Plasma Medicine 4 (2016) 19-28.
[5] A.C. Borges, K.G. Kostov, R.S. Pessoa, G. de Abreu, G.d.M. Lima, L.W. Figueira, C.Y.J.A.S. Koga-Ito, Applications of Cold Atmospheric Pressure Plasma in Dentistry, 11 (2021) 1975.
[6] N. O'connor, O. Cahill, S. Daniels, S. Galvin, H. Humphreys, Cold atmospheric pressure plasma and decontamination. Can it contribute to preventing hospital-acquired infections?, J. Hosp. Infect. 88 (2014) 59-65.
[7] S. Mitra, N. Kaushik, I.S. Moon, E.H. Choi, N.K. Kaushik, Utility of Reactive Species Generation in Plasma Medicine for Neuronal Development, Biomedicines 8 (2020) 348.
[8] K.S. Katiyar, A. Lin, A. Fridman, C.E. Keating, D.K. Cullen, V. Miller, Non-thermal plasma accelerates astrocyte regrowth and neurite regeneration following physical trauma in vitro, Applied Sciences 9 (2019) 3747.
[9] M. Keidar, D. Yan, I.I. Beilis, B. Trink, J.H. Sherman, Plasmas for treating cancer: opportunities for adaptive and self-adaptive approaches, Trends Biotechnol. 36 (2018) 586-593.
[10] A.M. Hirst, F.M. Frame, M. Arya, N.J. Maitland, D. O'Connell, Low temperature plasmas as emerging cancer therapeutics: the state of play and thoughts for the future, Tumor Biology (2016) 1-11.
[11] M. Khalili, L. Daniels, A. Lin, F.C. Krebs, A.E. Snook, S. Bekeschus, W.B. Bowne, V. Miller, Non-thermal plasma-induced immunogenic cell death in cancer, J. Phys. D: Appl. Phys. 52 (2019) 423001.
[12] M.H. Ngo Thi, P.L. Shao, J.D. Liao, C.C.K. Lin, H.K. Yip, Enhancement of Angiogenesis and Epithelialization Processes in Mice with Burn Wounds through ROS/RNS Signals Generated by Non‐Thermal N2/Ar Micro‐Plasma, Plasma Process Polym 11 (2014) 1076-1088.
[13] A. Lin, N. Chernets, J. Han, Y. Alicea, D. Dobrynin, G. Fridman, T.A. Freeman, A. Fridman, V. Miller, Non‐Equilibrium Dielectric Barrier Discharge Treatment of Mesenchymal Stem Cells: Charges and Reactive Oxygen Species Play the Major Role in Cell Death, Plasma Process Polym (2015).
[14] S. Bekeschus, K. Wende, M.M. Hefny, K. Rödder, H. Jablonowski, A. Schmidt, T. von Woedtke, K.-D. Weltmann, J. Benedikt, Oxygen atoms are critical in rendering THP-1 leukaemia cells susceptible to cold physical plasma-induced apoptosis, Scientific reports 7 (2017) 1-12.
[15] X. Lu, G. Naidis, M. Laroussi, S. Reuter, D. Graves, K. Ostrikov, Reactive species in non-equilibrium atmospheric-pressure plasmas: Generation, transport, and biological effects, Physics Reports 630 (2016) 1-84.
[16] A. Privat-Maldonado, A. Schmidt, A. Lin, K.-D. Weltmann, K. Wende, A. Bogaerts, S. Bekeschus, Ros from physical plasmas: Redox chemistry for biomedical therapy, Oxidative medicine cellular longevity 2019 (2019).

[17] D. Gidon, D.B. Graves, A. Mesbah, Effective dose delivery in atmospheric pressure plasma jets for plasma medicine: a model predictive control approach, Plasma Sources Science Technology 26 (2017) 085005.
[18] X. Lu, M. Laroussi, V. Puech, On atmospheric-pressure non-equilibrium plasma jets and plasma bullets, Plasma Sources Sci. Technol. 21 (2012) 034005.
[19] A. Fridman, A. Chirokov, A. Gutsol, Non-thermal atmospheric pressure discharges, J. Phys. D: Appl. Phys. 38 (2005) R1.
[20] S. Bekeschus, A. Lin, A. Fridman, K. Wende, K.-D. Weltmann, V. Miller, A Comparison of Floating-Electrode DBD and kINPen Jet: Plasma Parameters to Achieve Similar Growth Reduction in Colon Cancer Cells Under Standardized Conditions, Plasma Chem. Plasma Process. 38 (2018) 1-12.
[21] A. Lin, B. Truong, S. Patel, N. Kaushik, E.H. Choi, G. Fridman, A. Fridman, V. Miller, Nanosecond-Pulsed DBD Plasma-Generated Reactive Oxygen Species Trigger Immunogenic Cell Death in A549 Lung Carcinoma Cells through Intracellular Oxidative Stress, International Journal of Molecular Sciences 18 (2017) 966.
[22] S. Reuter, T. Von Woedtke, K.-D.J.J.o.P.D.A.P. Weltmann, The kINPen—a review on physics and chemistry of the atmospheric pressure plasma jet and its applications, 51 (2018) 233001.
[23] D. Dobrynin, G. Fridman, G. Friedman, A. Fridman, Physical and biological mechanisms of direct plasma interaction with living tissue, New Journal of Physics 11 (2009) 115020.
[24] A. Lin, Y. Gorbanev, J. De Backer, J. Van Loenhout, W. Van Boxem, F. Lemière, P. Cos, S. Dewilde, E. Smits, A. Bogaerts, Non‐Thermal plasma as a unique delivery system of short‐lived reactive oxygen and nitrogen species for immunogenic cell death in melanoma cells, Advanced Science 6 (2019) 1802062.
[25] L. Galluzzi, A. Buqué, O. Kepp, L. Zitvogel, G. Kroemer, Immunogenic cell death in cancer and infectious disease, Nature Reviews Immunology (2016).
[26] A. Lin, J. Razzokov, H. Verswyvel, A. Privat-Maldonado, J. De Backer, M. Yusupov, E. Cardenas De La Hoz, P. Ponsaerts, E. Smits, A. Bogaerts, Oxidation of Innate Immune Checkpoint CD47 on Cancer Cells with Non-Thermal Plasma, Cancers 13 (2021) 579.
[27] A. Lin, E. Biscop, C. Breen, S.J. Butler, E. Smits, A.J.O.m. Bogaerts, c. longevity, Critical Evaluation of the Interaction of Reactive Oxygen and Nitrogen Species with Blood to Inform the Clinical Translation of Nonthermal Plasma Therapy, 2020 (2020).
[28] E. Simoncelli, A. Stancampiano, M. Boselli, M. Gherardi, V. Colombo, Experimental investigation on the influence of target physical properties on an impinging plasma jet, Plasma 2 (2019) 369-379.
[29] A.G. Lin, B. Xiang, D.J. Merlino, T.R. Baybutt, J. Sahu, A. Fridman, A.E. Snook, V. Miller, Non-thermal plasma induces immunogenic cell death in vivo in murine CT26 colorectal tumors, Oncoimmunology 7 (2018) e1484978.
[30] M. Vandamme, E. Robert, S. Lerondel, V. Sarron, D. Ries, S. Dozias, J. Sobilo, D. Gosset, C. Kieda, B. Legrain, ROS implication in a new antitumor strategy based on non‐thermal plasma, International journal of cancer 130 (2012) 2185-2194.
[31] N. Chernets, D.S. Kurpad, V. Alexeev, D.B. Rodrigues, T.A. Freeman, Reaction Chemistry Generated by Nanosecond Pulsed Dielectric Barrier Discharge Treatment is Responsible for the Tumor Eradication in the B16 Melanoma Mouse Model, Plasma Process Polym (2015).
[32] P. Friedman, V. Miller, G. Fridman, A. Lin, A. Fridman, Successful Treatment of Actinic Keratosis Using Non-Thermal Atmospheric Pressure Plasma- A Case Series, J. Am. Acad. Dermatol. 76 (2017) 352-353.
[33] P. Friedman, V. Miller, G. Fridman, A.J.C. Fridman, e. dermatology, Use of cold atmospheric pressure plasma to treat warts: a potential therapeutic option, 44 (2019) 459-461.

[34] P.C. Friedman, G. Fridman, A.J.P.d. Fridman, Using cold plasma to treat warts in children: A case series, 37 (2020) 706-709.
[35] S. Kalghatgi, G. Friedman, A. Fridman, A.M. Clyne, Endothelial cell proliferation is enhanced by low dose non-thermal plasma through fibroblast growth factor-2 release, Annals of biomedical engineering 38 (2010) 748-757.
[36] K.P. Arjunan, G. Friedman, A. Fridman, A.M. Clyne, Non-thermal dielectric barrier discharge plasma induces angiogenesis through reactive oxygen species, Journal of the Royal Society Interface (2011) rsif20110220.
[37] A.A. Fridman, A. Lin, V. Miller, S. Bekeschus, K. Wende, K.-D.J.P.M. Weltmann, The plasma treatment unit: An attempt to standardize cold plasma treatment for defined biological effects, 8 (2018).
[38] H. Cheng, J. Xu, X. Li, D. Liu, X.J.P.o.P. Lu, On the dose of plasma medicine: Equivalent total oxidation potential (ETOP), 27 (2020) 063514.
[39] S.G. Joshi, M. Paff, G. Friedman, G. Fridman, A. Fridman, A.D. Brooks, Control of methicillin-resistant Staphylococcus aureus in planktonic form and biofilms: a biocidal efficacy study of nonthermal dielectric-barrier discharge plasma, Am. J. Infect. Control 38 (2010) 293-301.
[40] H.-R. Metelmann, D.S. Nedrelow, C. Seebauer, M. Schuster, T. von Woedtke, K.-D. Weltmann, S. Kindler, P.H. Metelmann, S.E. Finkelstein, D.D. Von Hoff, Head and neck cancer treatment and physical plasma, Clinical Plasma Medicine 3 (2015) 17-23.
[41] S. Vandersee, Clinical use of cold atmospheric pressure argon plasma in chronic leg ulcers: A pilot study, J. Wound Care 24 (2015) 196.
[42] M. Schuster, C. Seebauer, R. Rutkowski, A. Hauschild, F. Podmelle, C. Metelmann, B. Metelmann, T. von Woedtke, S. Hasse, K.-D. Weltmann, Visible tumor surface response to physical plasma and apoptotic cell kill in head and neck cancer, J Journal of Cranio-Maxillofacial Surgery 44 (2016) 1445-1452.
[43] H.-R. Metelmann, C. Seebauer, V. Miller, A. Fridman, G. Bauer, D.B. Graves, J.-M. Pouvesle, R. Rutkowski, M. Schuster, S. Bekeschus, Clinical experience with cold plasma in the treatment of locally advanced head and neck cancer, Clinical Plasma Medicine 9 (2018) 6-13.
[44] S.H. Benedict, K.M. Yenice, D. Followill, J.M. Galvin, W. Hinson, B. Kavanagh, P. Keall, M. Lovelock, S. Meeks, L. Papiez, Stereotactic body radiation therapy: the report of AAPM Task Group 101, Medical physics 37 (2010) 4078-4101.
[45] T. Depuydt, K. Poels, D. Verellen, B. Engels, C. Collen, C. Haverbeke, T. Gevaert, N. Buls, G. Van Gompel, T. Reynders, Initial assessment of tumor tracking with a gimbaled linac system in clinical circumstances: a patient simulation study, Radiotherapy and Oncology 106 (2013) 236-240.
[46] C.M. Ionescu, C. Copot, D. Verellen, Motion compensation for robotic lung tumour radiotherapy in remote locations: A personalised medicine approach, Acta Astronautica 132 (2017) 59-66.
[47] S. Sayeh, J. Wang, W.T. Main, W. Kilby, C.R. Maurer, Respiratory motion tracking for robotic radiosurgery, Treating tumors that move with respiration, Springer2007, pp. 15-29.
[48] A.D. Bonzanini, J.A. Paulson, D.B. Graves, A. Mesbah, Toward safe dose delivery in plasma medicine using projected neural network-based fast approximate NMPC, IFAC Proceedings Volumes, 2020.
[49] A.D. Bonzanini, K. Shao, A. Stancampiano, D.B. Graves, A. Mesbah, Perspectives on Machine Learning-assisted Plasma Medicine: Towards Automated Plasma Treatment, IEEE Transactions on Radiation Plasma Medical Sciences (2021).

SUPPORTING INFORMATION

Additional supporting information is available in the online version of this article at the publisher's website or from the author.

Graphical Abstract

The impact of total plasma treatment energy on chemical species generation and cancer cell viability was investigated *in vitro* using a microsecond-pulsed DBD system. Total treatment energy encompasses the influence of plasma application parameters: pulse frequency, treatment time, and application distance. Results here are strategic steps towards standardizing plasma treatment and dose.